Analele Universităţii din Oradea, Seria Geografie **XXXIV,** no. 2/**2024**, pp. 105-122
ISSN **1221-1273**, E-ISSN **2065-3409** DOI 10.30892/auog.34202-916

QUANTITATIVE ANALYSIS OF GEOMORPHIC RESPONSES AND TOPSIS APPROACHE ANALYSIS TO ACTIVE TECTONIC PROCESS: A CASE STUDY OF THE NORTHEAST OF THE AURES (TEBESSA)

Taib HASSAN*
University Frères Mentouri Constantine 1, Department of Geological Sciences,
Faculty of Earth Sciences, Geography and Regional Planning,
P.O. Box, 325 Ain El Bey Way, Constantine, 25017, Algeria;
Ferhat Abbas University, Laboratory of Applied Research in Engineering Geology, Geotechnics, Water Sciences, and Environment,19137, Setif, Algeria;
e-mail: hacen-taib68@gmail.com

Hadji RIHEB
Ferhat Abbas University, Department of Earth Sciences, Institute of Architecture and Earth Sciences, Laboratory of Applied Research in Engineering Geology, Geotechnics, Water Sciences, and Environment, 19137, Setif, Algeria;
e-mail: hadji.rihab@univ-setif.dz

Citation: Hassan T. & Riheb H. (2024). Quantitative analysis of geomorphic responses and and topsis approache analysis to active tectonic process: a case study of the northeast of the Aures (Tebessa). *Analele Universităţii din Oradea, Seria Geografie*, *34*(2), 105-122. https://doi.org/10.30892/auog.34202-916

Abstract: This study combines GIS and remote sensing technologies to analyze geomorphological changes in the Tebessa basin, focusing on key indices such as hypsometric integral (HI) and stream sinuosity (SS). The objective was to assess how drainage anomalies and tectonic activity influence flow and relief patterns. Asymmetry and topographic factors were incorporated into a geographic information system, and the region was classified into four IRAT classes: high, medium, low, and rank. Results identified highly deformed areas near active tectonic anomalies, highlighting subsurface fault activity and its influence on river sinuosity. A new diagram illustrates the spatial evolution of these structures, providing insight into the region's geological dynamics. The study also applied the TOPSIS method to prioritize watershed areas based on tectonic activity, offering a comprehensive analysis of the basin's geomorphological changes.

Key words: Geomorphometric, GIS, Morpho-structural, Tebessa,Tectonic

* Corresponding Author

* * * * * *

INTRODUCTION

The case study provides a quantitative analysis of the responses of geomorphic elements to the active tectonic processes in Algeria. The Tethys' closure during the Miocene-Lower Palaeocene period triggered the orogeny in the region. Following this collision, a new deformation zone emerged starting in Burdigalian. However, the exact number and timing of tectonic events in the region remain a topic of debate among researchers. Geological records have revealed previously unknown structures, including compression, distension, strike-slip fault systems, contributing to the area's complex tectonic framework. The collapse basins in Algeria highlight how significant the influence of the Earth's crust is on the development of the NE African Basin (Philip, et al., 1986; Chihi, 1988; Tamani, Hadji, Hamad, & Hamed, 2019; Taib, et al., 2023). The continuous effect of crustal dislocation persisted until the emergence of Pantelleria rift. During the Plio-Quaternary period, the region experienced an extensional tectonic event characterized by high-angle normal faults intersecting pre-existing structures, resulting in tectonic depressions. This research aims to elucidate the behaviour, dynamics of one such collapse basin within the Tebessa region. Given the area's geological significance and the intricate interplay between tectonic forces and geomorphic responses, a quantitative analysis of the geomorphic changes in the Tebessa region is of paramount importance. Understanding the dynamics, characteristics, interactions of active tectonic processes in this area will significantly enhance our knowledge of the region's geological evolution. It has practical implications for hazard assessment, land management strategies in the context of active tectonics. This comprehensive understanding of geomorphic responses facilitates better planning and mitigation strategies in regions affected by ongoing tectonic activity. The practical interest of this study lies in its potential to improve hazard assessment, land management strategies, contributing to more effective planning in tectonically active areas. Hypsometric analysis is an essential tool for assessing, comparing the geomorphic evolution of various landforms, regardless of the factors driving this evolution. In regions experiencing rapid uplift; the hypsometric integral (HI) shows a strong correlation with uplift rates. Differences in regardless of the factors that influence the geomorphic changes, the Hypsometric Analysis method is an ideal tool for studying and comparing the changes in landforms (Taib, et al., 2022), demonstrated through a mathematical model that the hypsometric curve depends on the drainage network, landscape runoff processes, basin geometry, that HI correlates positively with uplift rate.

GEOLOGICAL SETTING

The NE African Basin is located in the northeast part of the Aure Nememcha chain. It falls within the Saharan Atlas' North Auresian autochthon (Dubourdieu & Durozoy, 1950) (figure 1). The region's structural style is characterized by folds and faults in various directions. Analyzing geomorphic features like lineaments and drainage patterns provides insights into the region's tectonic setting and landscape evolution. Figure 3 displays a structural context depicting the NE-SW orientation of fold axes, with accompanying NW-SE oriented grabens. Numerous research studies have focused on the area, investigating various aspects such as geology, geomorphology, and the environment (Zeqiri, et al., 2019). The neotectonic aspect has not been specifically addressed in these studies. The Trias diapiric is responsible for the displacement of carbonate structures at Djebel Jebissa and Djebel Belekfif. The thick limestone-marl formations are visible along the borders. The contrasting features of these deposits, which are located in the Piedmonts, contrast the previous structures (Vila, 1980; Hadji, et al., 2014). The region is characterized by the presence of several collapsed Plio-Quaternary basins, some of which are located in Kasserine, Morsot-Tebessa-Hammamet, Sbiba-Cherichira, and Kalaa Djerad. However, limited research has been conducted on these basins in Algeria. According to a study (Hamad, et al., 2021), the formation of the Tebessa basin can be attributed to multiple faults, with the region exhibiting significant fractures that have shaped its current physiognomy.

Figure 1. Geographic location of the study area

The study area displays three primary lineaments: North-West-SouthEast, NorthEast-SouthWest and East-West. The two first are more prominent, while the others exhibit a relatively uniform distribution. Gravimetric data collected (Hamad, et al., 2021) indicate the presence of well-developed faults in the Tebessa basins. Mapped faults align with observed fractures (figure 3). Through field studies conducted in the Jebel Doukkane and Jebel Mestiri deposits, the researchers were able to gain a deeper understanding of the fractured index in the limestones of the Eocene and Cretaceous periods.

MATERIALS AND METHODS

They utilized various tools, such as geological and topographic maps, and Geographic Information Systems (GIS) to perform a comprehensive morphometric study of the region around Tebessa. By examining variations in hypsometric characteristics across different catchment areas, we identified clusters of high and low hypsometric values, evaluating their significance in relation to lithology and tectonics. This method has been used by several researchers in Neogene basins and has produced very realistic results (Taib, et al., 2022; Manchar, Hadji, Bougherara, & Boufaa, 2022). The morphometric indices were extracted from a 30m*30m Digital Elevation model, using ArcGIS 10.8 software. The computed geomorphological indices utilized in this research are based on well-established parameters commonly employed in similar studies (Keller & Pinter, 1996; Peters & Van Balen, 2007). These parameters include hypsometric integral, asymmetry factor, stream sinuosity, relative tectonic uplift, flux length gradient index, and basin elongation ratio index. By considering these indices, we aim to achieve a thorough analysis of the overall regional trend (Shamurailatpam, 2014; Esmaeil, et al., 2017; Ghedoui, 2014).

The methodology employed in this study has been successfully applied in various geological domains where active tectonics is present. For example, the researchers were able to analyze the Zagros center (Dehbozorgi, et al., 2010) and the North Rhine Graben using the Hypsometric Analysis method (Peters & Van Balen, 2007). Furthermore, this methodology has been applied to study the southwest Sierra Nevada in Spain (El Hamdouni, et al., 2008). By utilizing this established methodology and adapting it to our study area. The goal of the researchers is to provide a comprehensive analysis of the various active tectonic processes that are taking place in the area.

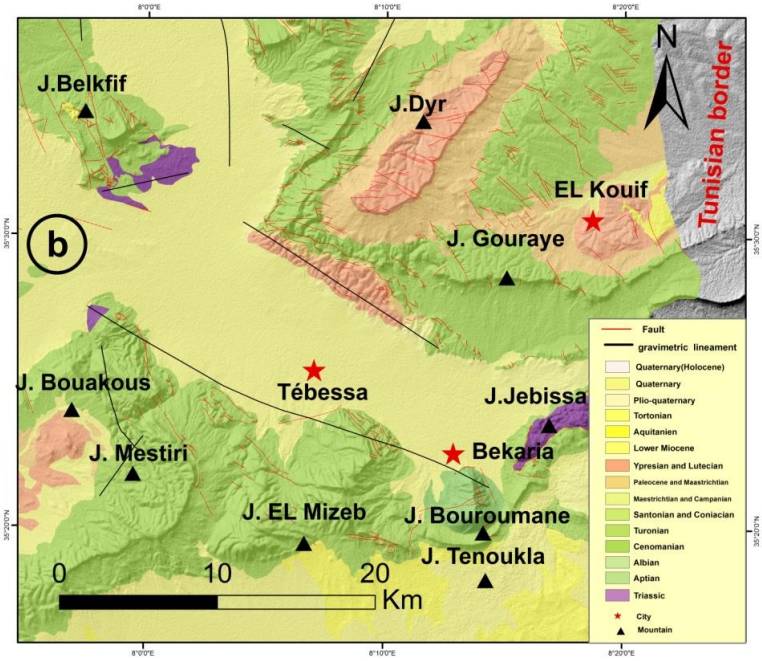

Figure 2. Stratigraphic simplified map of the study area

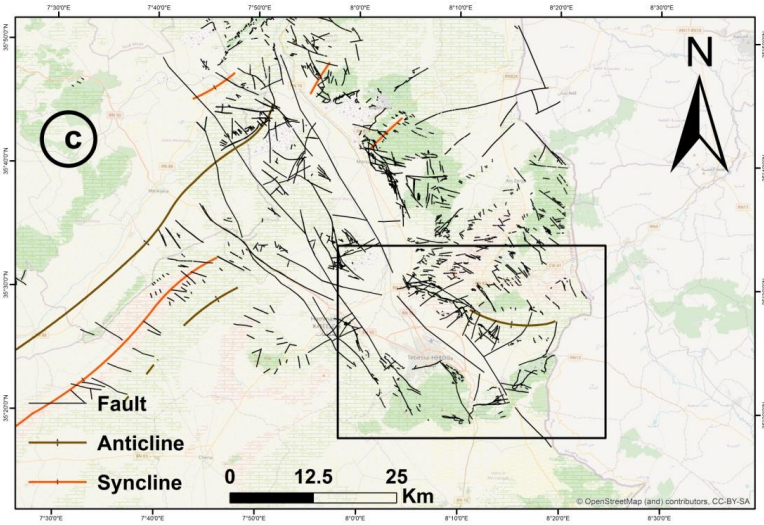

Figure 3. Structural map of the study area

Basin Prioritization by TopSIS Model

The researchers used the various parameters of the Tebessa basin to determine the level of activity. They then used the rankings to identify ideal and anti-ideal positions. The anti-ideal or optimal point can be determined by comparing the lower seismic activity values of SI or AF with those of these higher indices. The more active tectonic activities can also be observed if these two lower values are compared with those of the high activity tectonic. The ideal point is identified by the distance between the two solutions.

The researchers used Excel to perform a procedure that involved identifying the ideal point between two solutions **(Step 1**) (Aouragh & Essahlaoui, 2018). The researchers utilized the AHP to generate the TopSIS model's parameters. The alternatives were evaluated using the Xij criterion, while the C1 and C2 criteria were used to measure them. After the matrix was created, normalization exercises were then performed (**Step2**).

$$nij = \frac{Xij}{\left(\sqrt{\sum_{n=1}^{Xij} Xij^{2}}\right)} (equ\ 1)$$

The parameters used in the creation of the TopSIS model were derived by using the AHP.

Step 3. The weighted normalized value is calculated.

vij =wj ∗ nij, i=1,…,m, j=1,…, n (equ 2)

Step 4. The researchers then identified the ideal solutions based on the negative and positive criteria. the researchers used the classification method to identify the optimal positions.

$$W+= ((\max/i\ vij \mid J \in J), (\min/i\ vij \mid J \in J') \mid i = 1,2, \ldots\ldots, m) (equ\ 3)$$

$$= \{w_1^+ + w_2^+, \ldots\ldots, w_m^+ \}$$

$$W-= ((\min i\ wij \mid J \in J), (\max i\ vij \mid J \in J') \mid i = 1,2, \ldots\ldots, m) (equ\ 4)$$

$$= \{w_1^- + w_2^-, \ldots\ldots, w_m^- \}$$

Positive and negative criteria are associated with J and J′.

Step 5. involves dividing the distance between two points by taking into account the Euclidian dimension.

$$S_i^+ = \sqrt{\sum_{j=1}^{n}(w_i^+ + w_{ij})^2} \quad i = 1,2, \ldots\ldots, m (equ\ 5)$$

$$S_i^- = \sqrt{\sum_{j=1}^{n}(w_i^- - w_{ij})^2} \quad i = 1,2, \ldots\ldots, m (equ\ 6)$$

Step 6. Determine the relative closeness of the suggested solutions.

$$C_I^+ = \frac{S_i^+}{S_i^+ + S_i^-} (equ\ 7)$$

RESULTS

The Asymmetry Factor (Af):

Hare & Gardner introduced in 1985 the Asymmetry factor, which can be used to detect shifts in the direction of the drainage (figure 2).

$$\mathbf{AF} = (\mathbf{Ar} \div \mathbf{At}) \times \mathbf{100}$$

At: watershed total surface**; Ar:** right bank watershed surface

To avoid confusion between the different catchment areas, the absolute value of Af is used (Pérez-Peña, Azor, Azañón, & Keller, 2010).

$$\mathbf{AF} - \mathbf{50} = |50 - (\mathbf{Ar} \times 100) \div \mathbf{At}|.$$

Figure 4 shows the spatial distribution of asymmetrical factors in different watersheds. They are indicated as follows: moderately asymmetrical Af = 10-15, slightly symmetrical Af = 5 and strongly symmetrical Af = 15. Figure 4 shows the average values of the various catchment areas within the study area. They indicate that the highest values are in the areas between 17 and 24. Accidents NE-SW, E-W, and NW-SE directions within the graben borders can also be associated with these values.

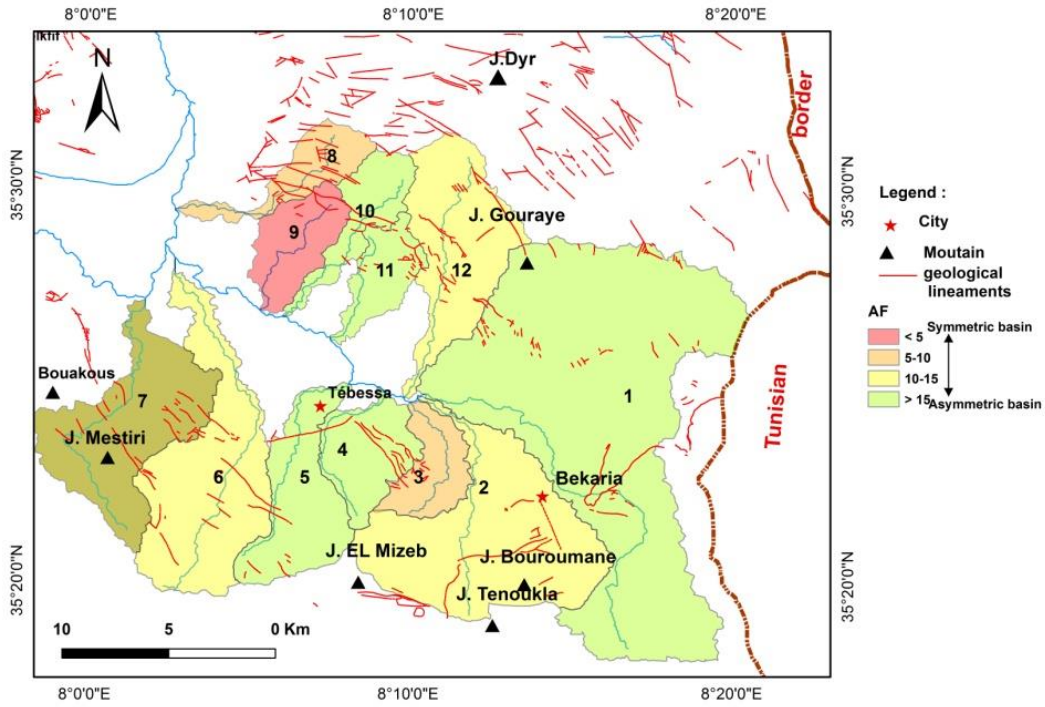

Figure 4. Geomorphometric Asymmetry Index Distribution Map AF

Hypsometric Integrals (Hi):

The hypsometric curve of a watershed is shown in figure 5. According to Kusre (2013) & Strahler (1952), the altitude can influence the distribution of a watershed's hypsometric curve. Its shape allows one to determine the area's degree of evolution and maturity.

The hypsometric curves and integrals of watersheds are also determined by the different age groups and processes of erosion.

The mature advanced basins' integrals and curves are regarded as the most accurate indicators of erosion's various phases. On the other hand, the immature basins' integrals and curves are interpreted differently. The hypsometric index is a type of calculation that shows the curve's shape.

The integral hypsometry index is a calculation that shows the shape of a hypsometric curve (Keller & Pinter, 2002; Kusre, 2013):

$$\mathbf{Hi} = ((\mathbf{Hmean} - \mathbf{Hmin}) \div (\mathbf{Hmax} - \mathbf{Hmin}))$$

A quantitative analysis of the drainage basin evolution was performed by Kusre (2013) & Strahler (1952). All sub-basins (figure 3) within the study area were analyzed using a single family with a specific interval and shape (Hi~ 0.5).

The researchers focused on the relationship between the various control parameters of a drainage basin and its hypsometric integral. They discovered that the high values exhibited by the integral can trigger a rejuvenation of the area's relief.

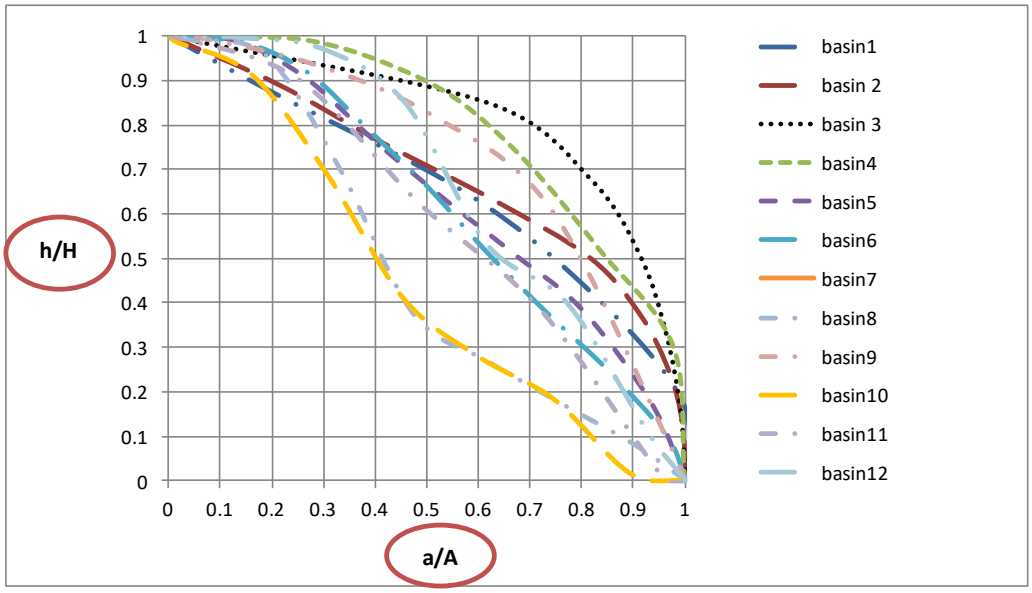

Figure 5. The hypsometric curves

Relative Tectonic Uplift

According to Singh & Jain (2009), the concept of an uplift(U) index was proposed to help in the evolution of the active tectonics in a given catchment area.

$$\mathbf{U} = \boldsymbol{hm} + (\mathbf{1} - \mathbf{HI})$$

where, **hm** is the average elevation of the catchment and **HI** is the integral hypsometry.

The values of relative tectonic upflit in all basins between (1.276-1.609). This index is divide into 2 Class (U <1) that's associated with slight uplift or influence of lithological and (U>1), that's associated with strongly uplifted block, which are located in areas that have recently undergone vertical movement, indicate that the erosion rate has reached the base level. This is due to the relative tectonics in the region (Keller & Pinter, 2002; Bull, 2007). The index has been used to calculate the UP index for various mounting fronts in the study area (Silva, Goy, Zazo, & Bardají, 2003; Pedrera, et al., 2009) For instance, the index for the whole basin is characterized by strongly uplifted block.

Stream sinuosity (SS)

The stream sinuosity can be used to evaluate an area's tectonic activity. It can be calculated by comparing the length of streams with the length of the curvilinear paths or the straight lines connecting the two ends of a channel.

$$SS = \frac{CL}{L}$$

The length of the channel is shown as CL, while the line connecting it to the other ends is L. A high SS value indicates that the river has become stable and is close to equilibrium. On the other hand, a low SS value indicates that the basin is active (Mueller, 1968). The value of SS < 1.05 represent tectonic activity, 1.05 < SS < 1.5 are semi-active and SS > 1.5 are inactive (Bull & McFadden, 1977). In the present study, the minimum value of the SS index is 1.011 for basin 2, and the maximum value is 1.589 for basin 7. The values were classified into hree classes (Mohsen, Ali, Mahmoud, & Mehran, 2020), i.e., Class 1 (1.011–1.174), Class 2 (1.175–1.280), and Class 3 (1.280–1.589) and spatially distributed. Table 1 provides a summary of the geomorphic indices of each of the twelve basins.

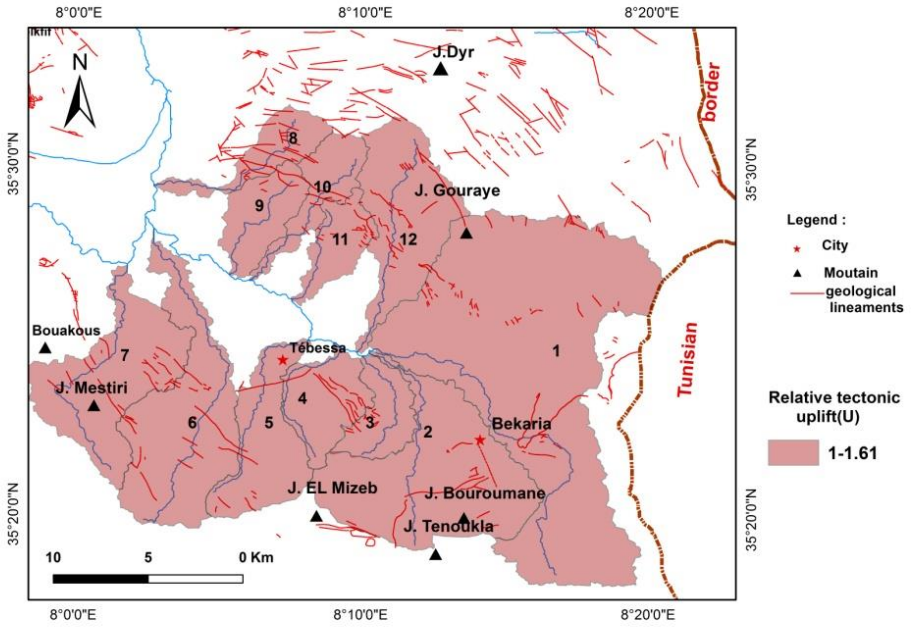

Figure 6. The Relative tectonic uplift index distribution map (U)

Flux Length Gradient Index (SL) (Hack, 1973): The channel slope index, which can be sensitive, can allow for the evolution of features in response to tectonics or rock resistance (Keller & Pinter, 2002).

$$SL = (\Delta H)/(\Delta L)/L$$

$(\Delta H)/\Delta L)$: stream segment slope

L: entire distance from the source to the middle of the segment under study

The SL index's value can also vary depending on the area's rock resistance. For instance, its value can increase in areas that have high rock resistance while it can decrease in lower rock resistance zones. A qualitative map of this type of rock was then generated (Keller & Pinter, 2002). The four different rock resistance levels are indicated in figure 9. They are very high, moderate, low, and moderate. The soil resistance level is also classified into three classes based on the data presented in figure 8. The lowest level is shown in the basin 9, while the maximum is in basin 6. The study area has been divided into two-class SL categories, with the highest values being recorded in basin 7. These categories correspond to the area's high rock resistance, which is mainly composed of natural limestone. These high values can be linked to the region's tectonic activities. Some of these are attributed to the area's interaction with different types of limestone and clay.

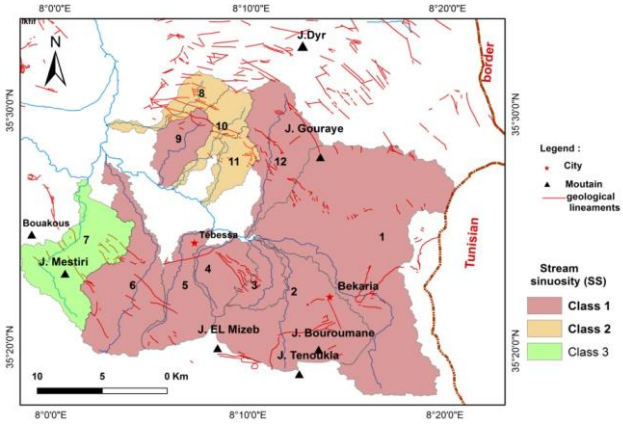

Figure 7. Stream sinuosity Index Distribution Map (SS)

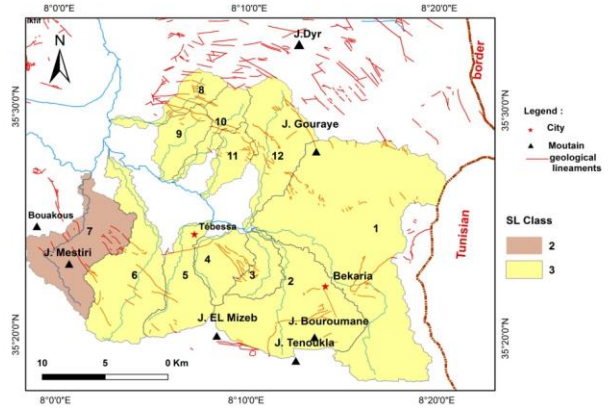

Figure 8. SL Index Class Distribution Map

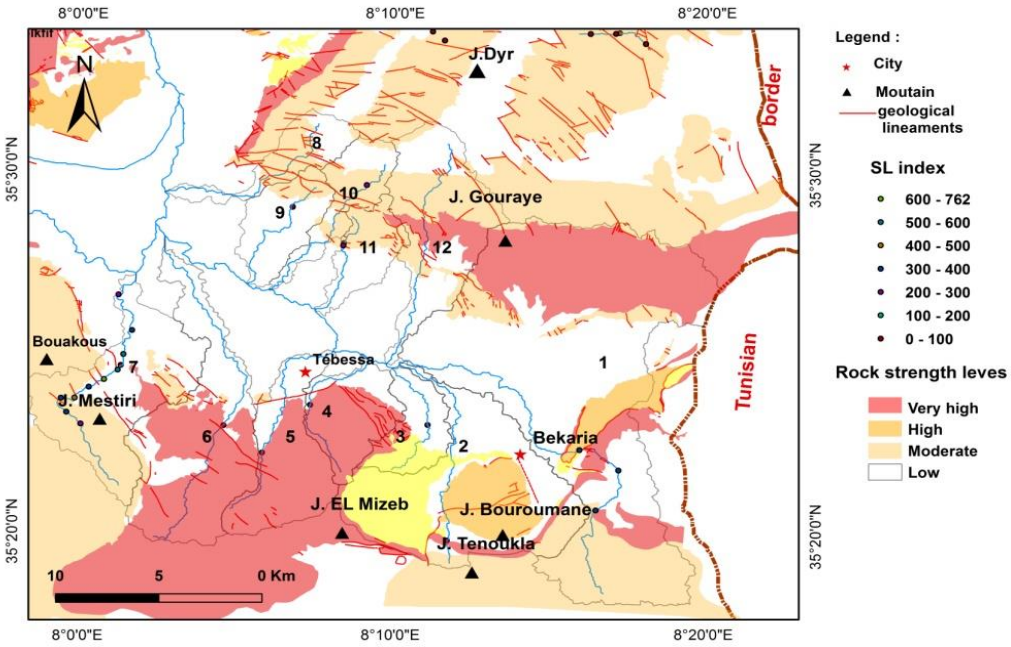

Figure 9. The Rock Resistance and SL index Map

Basin elongation ratio (BE)

The shape of the basin has changed due to its elongation ratio, which now exhibits a circular shape. The extension and rate of the area can be calculated to determine its projected shape:

$$\mathbf{BE} = \mathbf{2}\left(\frac{\boldsymbol{A}}{\boldsymbol{\pi}}\right)^{\mathbf{0.5}} \mathbf{/BL}$$

A: the area of basin

BL: maximum length of the basin

The high value of the index can be attributed to the existence of elongated pools near mountain fronts, which are known to rise and fall due to the natural break method. As stated by Chang et al. (2015), there are classified into 3 class namely Bs. Class 1(BE > 0.5) tectonically active areas, Class 2 (0.5< BE< 0.75) slightly active, and Class 3 (BE < 0.75) r inactive tectonic regions.

Figures 8 show the values of BE for different catchment areas within the study area. They show that the activities within these catchments are categorized into three classes: moderate, high, and low Activity tectonic as Class 1 (0.121-0.484), Class 2 (0.485-0.605), Class 3 (0.606-1694), in that order.

Accidents in the graben borders in the NE-SW, E-W and NW-SE directions coincide with these values. The values of BE for different graben borders are shown in figure 10. The highest one is in the 3rd basin, while the lowest one is in the 1st basin.

Transverse Topographic Symmetry Factor (T)

The quantity of the main stream is a factor that determines the asymmetry of its flow in a watershed. This is done by taking into account the varying characteristics of the different sections of the watershed.

$$T = Da / Dd$$

Da: Distance from the generator of the basin to the main river.
Dd: distance from the middle to the water-sharing line.

This measure is classified into three categories: class 1 (T 0.4), class 2 (0.4<T<0.2), and class 3 (T 0.2). The index's T-values are also consistent with the AF-values, which show the symmetry and inclination of the river's transverse topography (figure 11).

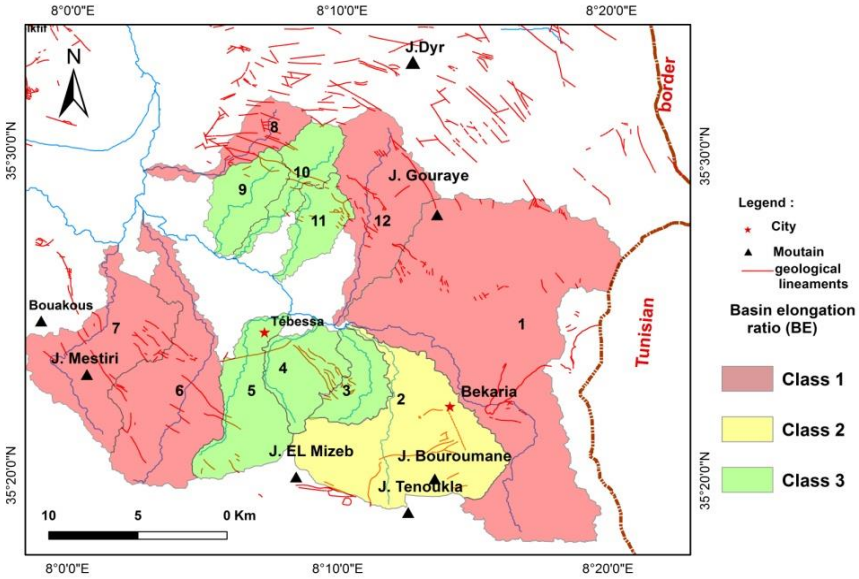

Figure 10. Map of BE Index Class Distribution

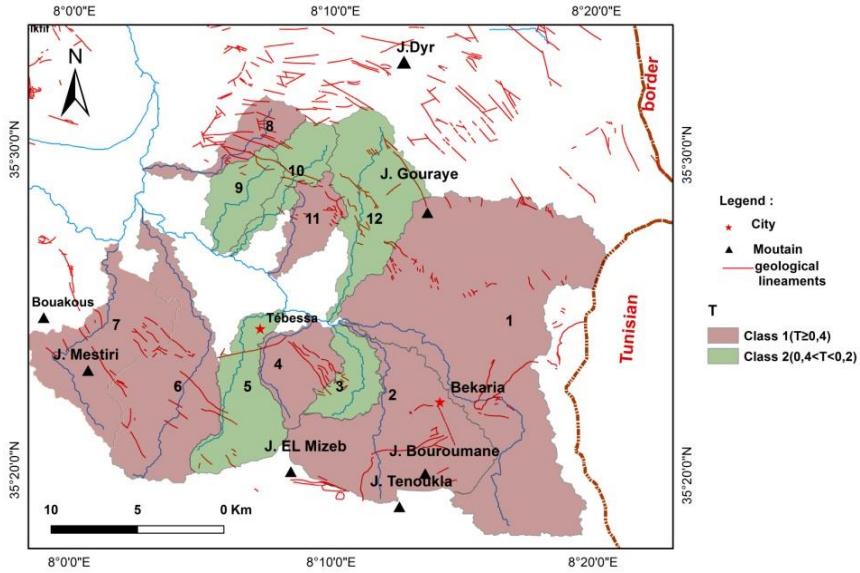

Figure 11. Map of Distribution of T-Index Classes

DISCUSSIONS

Understanding the relationship between geomorphology and neo-tectonic activity can provide valuable insight into the development of tectonic activities. A morpho-structural maps can also help identify the various structures and elements within a region. For instance, the mountainous area shows a significant distribution of morphological elements.

Due to the recent and current tectonic activities in the region, it is difficult to determine the exact levels of these marl masses. The findings of this study can also be used to identify the factors that triggered the development of the collapsed basin. The case of the Oued El Ksob valley, which is located in the Tebessa region, is a good example of the recent activity in the collapsed ditch. The numerous accidents that have been detected intersect the formation of the collapse ditch's plio-quaternary structures.

Table 1. Values of morphotectonic indices for the different watersheds studied
(Data source: Taib Hassan)

Basin	HI	AF	AF-50	BE	SS	Mean SL	Mean T	U
1	0,5	12,75	-37,25	0,121	1,053	151,59	0,63	1,276
2	0,49	35,33	-14,67	0,605	1,011	100,69	0,45	1,336
3	0,47	55,12	5,12	1,694	1,043	93,78	0,23	1,355
4	0,48	12,48	-37,52	1,331	1,048	122,29	0,82	1,337
5	0,5	15,39	-34,61	0,627	1,100	135,36	0,38	1,328
6	0,5	63,09	13,09	0,242	1,042	205,76	0,52	1,323
7	0,5	29,47	-20,53	0,15	1,589	303,74	0,56	1,325
8	0,49	56,33	6,33	0,25	1,280	172,83	0,83	1,333
9	0,49	48,57	-1,43	1,21	1,076	72,47	0,32	1,331
10	0,49	32,79	-17,21	0,847	1,120	161,51	0,39	1,488
11	0,5	85,97	35,97	1,33	1,257	100,48	0,4	1,332
12	0,5	61,13	11,13	0,484	1,174	115,63	0,37	1,609

IRAT Assessment and Discussion

The study area, which spans 12 sub-basins, is composed of various valleys. The quantitative and qualitative analysis of the IRAT of our region is carried out through the combination of the drainage and geo-morphometric indices. This allows us to identify anomalous features in the river system and the mountain fronts.

The identification of the drainage anomalies was carried out using the topographic factor index (T). This allows us to determine the hydrographic network's deviation and its relative asymmetry. The other component of the study is the determination of morphometric anomalies. These were derived from the Relative tectonic uplift (U) and (Hi) indices. The yield and IRAT of the seven calculated indices were then combined to determine the distribution of tectonic activity within the study area. Three classes of IRAT values were then established. The average of the seven geomorphic indices, which include the U, SS, Af, BE, SL, Hi, and T (table 1), was then used to determine the distribution of tectonic activity within the study area. The resulting index, which is a modified active tectonic index, was then classified into four classes (table 2). The first class was established as very high (1 Iat < 1.5), and by 2 high (1.5 <Iat < 2), 3 moderate (2 <Iat< 2.5), and 4 low (2.5< Iat) (El Hamdouni, Irigaray, Fernández, Chacón, & Keller, 2008).

Figure 12 shows the distribution of the four classes. The moderate and high Iat values dominate the map.

Table 2. Iat classification (relative tectonic activity index) in sub-basins
(Data source: Taib Hassan)

Basin	Class of							S/n	IATclass	Assessments
	SL	BE	AF	HI	U	T	SS			
1	3	1	1	2	1	1	1	1.429	1	**Very high**
2	3	2	2	2	1	1	1	1.714	2	**High**
3	3	3	2	2	1	2	1	2.000	2	**High**
4	3	3	1	2	1	1	1	1.714	2	**High**
5	3	3	1	2	1	2	1	1.857	2	**High**
6	3	1	2	2	1	1	1	1.571	2	**High**
7	2	1	2	2	1	1	3	1.714	2	**High**
8	3	1	2	2	1	1	2	1.714	2	**High**
9	3	3	3	2	1	2	1	2.143	3	**Moderately**
10	3	3	2	2	1	2	2	2.143	3	**Moderately**
11	3	3	1	2	1	1	2	1.857	2	**Moderately**
12	3	1	2	2	1	2	1	1.714	3	**Moderately**

Table 3 displays the decision matrix' weighted average according to the equation Eq. (2), wherein the W+ ideal solution takes into account the criterion's best performance, and the W- is derived from its poor output.

Table 3. Normalized matrix of morphometric pparameters of sub-basins
(Data source: Taib Hassan)

Basin	ER	AF	HI	UP	T	SL	SS
1	0.00107	0.00476	0.00253	0.02104	0.02776	0.00436	0.00992
2	0.00538	0.01320	0.00248	0.02203	0.01983	0.00289	0.00952
3	0.01507	0.02059	0.00238	0.02234	0.01013	0.00270	0.00983
4	0.01184	0.00466	0.00243	0.02204	0.03613	0.00352	0.00988
5	0.00646	0.00575	0.00253	0.02189	0.01674	0.00389	0.01036
6	0.00215	0.02357	0.00253	0.02181	0.02291	0.00592	0.00981
7	0.00133	0.01101	0.00253	0.02185	0.02467	0.00874	0.01497
8	0.00222	0.02105	0.00248	0.02198	0.03657	0.00497	0.01206
9	0.01076	0.01815	0.00248	0.02194	0.01410	0.00208	0.01013
10	0.00753	0.01225	0.00248	0.02453	0.01718	0.00465	0.01055
11	0.01183	0.03212	0.00253	0.02196	0.01762	0.00289	0.01184
12	0.00430	0.02284	0.00253	0.02653	0.01630	0.00333	0.01106

Table 4. Positive-ideal (W+) and negative-ideal (W-) solutions
(Data source: Taib Hassan)

Basin	ER	AF	HI	UP	T	SL	SS
W+	0.015074	0.032127	0.002538	0.026533	0.036576	0.008747	0.009529
W-	0.001076	0.004663	0.002385	0.021041	0.010135	0.002087	0.014979

Table 4 presents the two kinds of ideal solutions for a given criterion. These are denoted by the W+ and the W-. The comparability index's values can be calculated taking into account the alternatives. The priority list is sorted in ascending order. The results of the various sub-watersheds are obtained by equation Eq. (5.6. and 7) and presented in table 5. The scores ranged from 1.0099 to 1.0314, with the lowest being for the weakest sub-watershed and the highest for the strongest one.

Table 5. Prioritization of Tectonic activeness by Model TOPSIS
(Data source: Taib Hassan)

Basin	SI+	SI-	CI+	Rank Priority
1	0.0327391	0.01848066	1.01848066	7
2	0.02805236	0.01472451	1.01472451	10
3	0.02976989	0.02187313	1.02187313	5
4	0.02850342	0.02865327	1.02865327	3
5	0.03476836	0.00996043	1.00996043	12
6	0.02137697	0.02375281	1.02375281	4
7	0.02877158	0.01723076	1.01723076	9
8	0.01814351	0.03141157	1.03141157	1
9	0.02801351	0.01777075	1.01777075	8
10	0.02914726	0.01368983	1.01368983	11
11	0.02073828	0.03061783	1.03061783	2
12	0.02539166	0.02064203	1.02064203	6

The Topsis model take into account the tectonic activity of the watersheds and ranks them according to their active and passive status. For instance, the subbasin 8 and 5 are regarded as the least active and most active (figure 13).

The gols of the TopSIS methods is to identify watersheds that are affected by the tectonic changes that have occurred in their region (Kale, Sengupta, Achyuthan, & Jaiswal, 2014), along with colleagues, utilized the IAT to classify the different sub-basins into their respective categories.

The TopSIS framework can be utilized to rank the different types of watersheds according to their relative activeness and performance. It can be additionally used to group them into a single category. According to the researchers, the model's simple and logical design makes it an ideal tool for users to solve their problems.

Among the disadvantages of the TopSIS system is its capability to alter the order of rank by removing or adding alternatives. This method can lead to a total rank reversal, as the previous option becomes known as the worst after being regarded as the best.

CONCLUSIONS

The morphometric indices utilized in this investigation to assess the rate of erosion and tectonic activity in the Tebessa study area include Sl, BE, SS, Hi, Af, U, and T. The analysis of HI values reveals a convex to sub-rectilinear shape, while SL anomalies are typically observed in the fault zone. The high U values (U > 1) indicate that tectonic activity is influenced by relative tectonics. Moreover, the sinuosity observed in Smf values along the fault suggests the presence of tectonic activity. The significantly higher asymmetrical factor, exceeding 50, indicates a high level of tectonic activity in the study area. Additionally, the calculated T-values corroborate the presence of relatively high tectonic activity. However, Class 1 BE values demonstrate localized tectonic activity in certain parts of the study area, while Classes 2 and 3 exhibit more dispersed occurrences elsewhere.

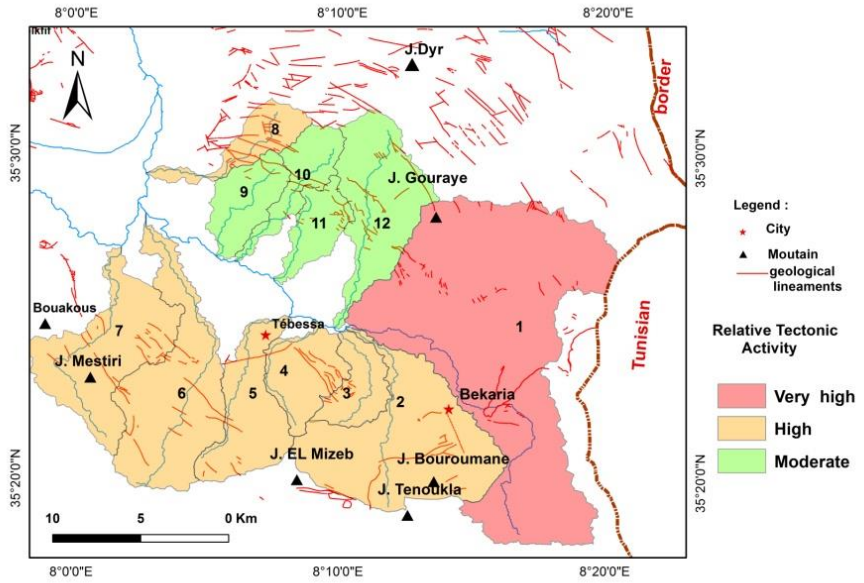

Figure 12. Tectonic activity index (IRAT) Map

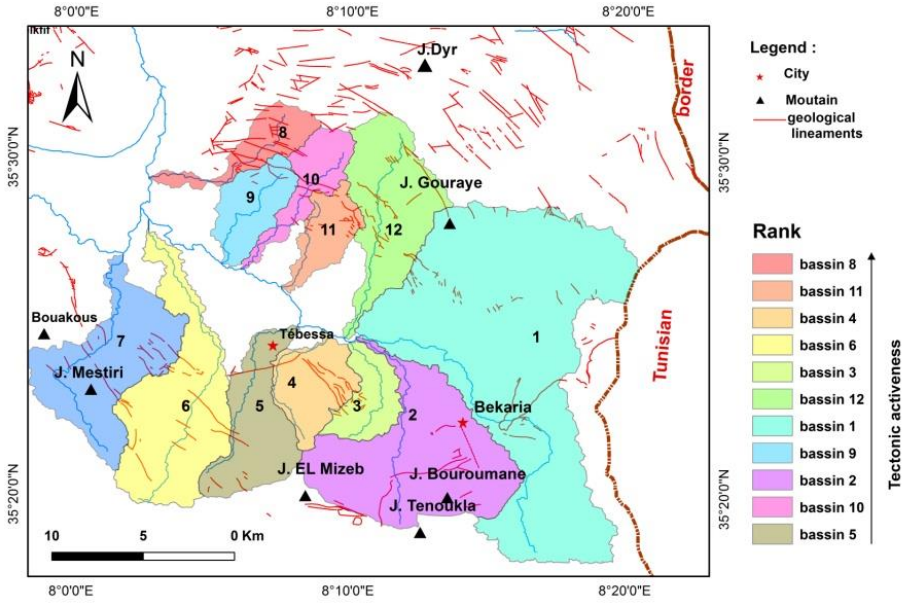

Figure 13. Ranking of the 12 watersheds of Tebessa by model TOPSIS

Throughout the study, comprehensive spatial data preparation was conducted, and the Geographic Information System (GIS) was employed for the analysis. These procedures facilitated the examination of various morphometric records and the evaluation of the impacts of tectonic activities on the landscape. Furthermore, they facilitated the investigation of the relationship between tectonic-geomorphological and hydrographic characteristics in the study area.

The morphometric indices employed in this study provided valuable insights into the rate of erosion and tectonic activity in the watershed. The results indicated the influence of tectonic forces on the landscape, as evidenced by the observed patterns and anomalies in the morphometric data. The integration of GIS technology and the analysis of spatial data proved to be essential in unraveling the complex relationship between tectonic processes and geomorphological features. The findings contribute to our understanding of active tectonics in the study area and provide a foundation for further research and monitoring efforts. The use of RS tools and GIS for prioritizing watersheds can be very simple and cost-effective. The TOPSIS approach can also help decision-makers develop activity tectonics.

REFERENCES

Aouragh, H., & Essahlaoui, A. (2018). A TOPSIS approach-based morphometric analysis for sub-watersheds prioritization of high Oum Er-Rbia basin, Morocco. *Spatial Information Research, 26* (2), 187–202. doi:https://doi.org/10.1007/s41324-018-0169-z

Azor, A., Keller, E. A., & Yeats, R. S. (2002). Geomorphic indicators of active fold growth: South Mountain–Oak Ridge anticline, Ventura basin, southern California. *Geological society of America bulletin, 114* (6), 745-753. doi:https://doi.org/10.1130/0016-7606(2002)114 <0745 :GIOAFG>2.0.CO;2

Benabbas, C. (2006). *Mio-Plio-Quaternaire des bassinscontinentaux de l'Algérienordorientale: apport de la photogéologie et analyse morpho structurale. Thèse de doctorat, Univ. Mentouri Constantine.* Constantine.

Bull, W. B. (2007). *Tectonic geomorphology of mountains: a new approach to paleoseismology.* Australia: Blackwell.

Bull, W. B., & McFadden, L. D. (1977). Tectonic geomorphology north and south of the Garlock fault, California. In *Geomorphology in arid regions* (pp. 115-138). Routledge.

Chihi, L. (1988). Déformations tectoniques quaternaires en Tunisie centrale (région de Kasserine). *Géologie Méditerranéenne, 15* (3), 177-182.

Dehbozorgi, M., Pourkermani, M., Arian, M., Matkan, A., Motamedi, H., & Hosseiniasl, A. (2010). Quantitative analysis of relative tectonic activity in the Sarvestan area, central Zagros, Iran. *Geomorphology, 121* (3-4), 329-341. doi:https://doi.org/10 .1016/j. geomorph .2010.05.002

Dubourdieu, G., & Durozoy, G. (1950). Observations tectoniques dans les environs de Tébessa et de l'Ouenza (Algérie). *Bulletin de la Société géologique de France, 5* (4-6), 257-266.

Durand, D. (1980). *La Méditerranée occidentale : étape de sa genèse et problèmes structuraux liés à celle-ci.* (Vol. 10). France: Mémoire hors série de la Société Géologique de France.

El Hamdouni, R., Irigaray, C., Fernández, T., Chacón, J., & Keller, E. (2008). Assessment of relative active tectonics, southwest border of the Sierra Nevada (southern Spain). *Geomorphology, 96* (1-2), 150-173. doi:https://doi.org/10.1016/j.geomorph.2007.08.004

Esmaeil, H. E., Solgi, A., Pourkermani, M., Matkan, A., & Mehran, A. (2017). Assessment of relative active tectonics in the Bozgoush basin (SW of Caspian Sea). *Open Journal of Marine Science, 7* (2), 211-237. doi:https://doi.org/ 10.4236/ojms.2017.72016

Ghedoui, R. (2014). *apports de l'image sismique et des SIG à l'étude morphostructurale de la Jeffara (Sud Est Tunisien): Implicationsgéodynamiques et intérets pétroliers.* Paris: Université Paris-Esr Marne La Vallée.

Hack, J. T. (1973). Stream-profile analysis and stream-gradient index. *Journal of Research of the us Geological Survey, 1* (4), 421-429.

Hadji, R., Limani, Y., Boumazbeur, A. E., Demdoum, A., Zighmi, K., Zahri, F., et al. (2014). Climate change and its influence on shrinkage–swelling clays susceptibility in a semi-arid zone: a case study of Souk Ahras municipality, NE-Algeria. *Desalination and Water Treatment, 52* (10-12), 2057-2072. doi:https://doi.org/ 10.4236/ojms.2017.72016

Hamad, A., Hadji, R., Boubaya, D., Brahmi, S., Baali, F., Legrioui, R., et al. (2021). Integrating gravity data for structural investigation of the Youkous-Tebessa and Foussana-Talah transboundary basins (North Africa). *Euro-Mediterranean Journal for Environmental Integration, 6*, 1-11. doi:https://doi.org/ 10.1007/s41207-021-00270-7

Hare, P., & Gardner, T. (1985). Geomorphic indicators of vertical neotectonism along converging plate margins. Tectonic Geomorphology. *In Proceedings of the 15th Annual Binghamton Geomorphology Symposium*, (pp. 123-134). Boston, Allen and Unwin.

Kale, V., Sengupta, S., Achyuthan, H., & Jaiswal, M. K. (2014). Tectonic controls upon Kaveri River Drainage, Cratonic Peninsular India: Inferences from longitudinal profiles, morphotectonic indices, hanging valleys and fluvial records. *Geomorphology, 227*, 153–165.

Keller, E., & Pinter, N. (1996). *Active tectonics : earthquakes, uplift, and landscape.* (P. Hall, Ed.) New JerseyÉtats-Unis): Upper Saddle River .

Keller, E., & Pinter, N. (2002). *Active Tectonics, Earthquakes, Uplift and Landscape* (2nd Edition ed.). Upper Saddle River: Prentice Hall.

Kowalski, W. M., Hamimed, M., & Pharisat, A. (2002). Les étapes d'effondrement des grabens dans les confines algéro-tunisiens. *Bulletin du Service Géologique de l'Algérie, 13* (2), 131–152.

Kusre, B. (2013). Hypsometric analysis and watershed management of Diyung watershed in north eastern India. *Journal of the Geological Society of India, 82*, 262-270. doi:https://doi.org/ 10.1007/s12594-013-0148-x

Manchar, N., Hadji, R., Bougherara, A., & Boufaa, K. (2022). Assessment of relative-active tectonics in Rhumel-Smendou basin (NE Algeria) – observations from themorphometric indices and hydrographic features obtained by the digital elevation model. *Geomatics, Landmanagement and Landscape* (4), 47-65. http://dx.doi.org/10.15576/GLL/2022.4.47

Mueller, J. (1968). An Introduction to the Hydraulic and Topographic Sinuosity Indexes. *Annals of the Association of American Geographers* (58), 371-385.

Pedrera, A., Pérez-Peña, J. V., Galindo-Zaldívar, J., Azañón, J. M., & Azor, A. (2009). Testing the sensitivity of geomorphic indices in areas of low-rate active folding (eastern Betic Cordillera, Spain). *Geomorphology, 105* (3-4), 218-231. doi:https://doi.org/ 10.1016/j.geomorph.2008.09.026

Pérez-Peña, J. V., Azor, A., Azañón, J. M., & Keller, E. A. (2010). Active tectonics in the Sierra Nevada (Betic Cordillera, SE Spain): Insights from geomorphic indexes and drainage pattern analysis. *Geomorphology, 191* (1-2), 74-87. doi:https://doi.org/ 10.1016/j.geomor ph.2010.02.020

Peters, G., & Van Balen, R. (2007). Pleistocene tectonics inferred from fluvial terraces of the northern Upper Rhine Graben, Germany. *Tectonophysics, 430* (1-4), 41-65. doi:https://doi.org/10.1016/j.tecto.2006.10.008

Philip, H., Andrieux, J., Dlala, M., Chihi, L., & Ben Ayed, N. (1986). Moi-plio quaternary tectonic evolution of the Kasserine grabene (Central Tunisia)-Implications of recent geodynamic evolution of Tunisia. *Bulletin de la Société géologique de France, 2*(4), 559-568. doi:https://doi.org/ 10.2113/gssgfbull.II.4.559

Silva, P. G., Goy, J., Zazo, C., & Bardají, T. (2003). Fault-generated mountain fronts in southeast Spain: geomorphologic assessment of tectonic and seismic activity. *Geomorphology, 50* (1-3), 203-225. doi:https://doi.org/ 10.1016/S0169-555X(02)00215-5

Singh, T., & Jain, V. (2009). Tectonic constraints on watershed development on frontal ridges: Mohand Ridge, NW Himalaya, India. *Geomorphology, 106* (3-4), Geomorphology. doi:https://doi.org/ 10.1016/j.geomorph.2008.11.001

Strahler, A. (1952). Hypsometric (area-altitude) analysis of erosional topography. *Geological society of America bulletin, 63* (11), 1117-1142.

Strahler, A. N. (1957). Quantitative analysis of watershed geomorphology. *Eos, Transactions American Geophysical Union, 38* (6), 913-920.

Taib, H., Benabbas, C., Khiari, A., Hadji, R., & Dinar, H. (2022). Geomatics-based assessment of the Neotectonic landscape evolution along the Tebessa-Morsott-Youkous collapsed. *Geomatics, Landmanagement and Landscape, (*3), 131-146. http://dx.doi.org/10.15576/GLL/2022.3.131

Taib, H., Hadji, R., & Hamed, Y. (2023). Erosion patterns, drainage dynamics, and their environmental implications: a case study of the hammamet basin using advanced geospatial and morphometric analysis. Journal of Umm Al-Qura University for Applied Sciences, 1-16.

Tamani, F., Hadji, R., Hamad, A., & Hamed, Y. (2019). Integrating remotely sensed and GIS data for the detailed geological mapping in semi-arid regions: case of Youks les Bains Area, Tebessa Province, NE Algeria. *Geotechnical and Geological Engineering, 37* (4), 2903-2913. doi:https://doi.org/10.1007/s10706-019-00807-2

Taesiri, V., Mohsen, P., Ali, S., Mahmoud, A., & Mehran, A. (2020). Morphotectonics of Alborz Province (Iran): A Case Study Using GIS Method. *Geotectonics, 54* (5), 691-704. doi:https://doi.org/10.1134/S001685212005009X

Vila, J. (1980). *The alpine chain of eastern Algeria and the Algerian-Tunisian borders.* Paris: Pierre and Marie Curie University.

Wildi, W. (1983). *The Tello-Rif chain (Algeria, Morocco, Tunisia): stratigraphic structure and evolution from the Triassic to the Miocene.* France.

Zeqiri, R. R., Riheb, H., Zighm, K., Guesmi, Y., Boudjellal, R., & Mahleb, A. (2019). Analysis of safety factor of security plates in the mine" Trepça" Stantërg. *Mining Science, 26*, 21-36. doi:https://doi.org/10.37190/msc192602

Submitted: April 23, 2024 | Revised: October 23, 2024 | Accepted and published online: October 29, 2024